JOURNAL OF PHYSICAL ORGANIC CHEMISTRY, VOL. 11, 232–240 (1998)

Molecular Orbital Calculations on the P—S Bond Cleavage Step in the Hydroperoxidolysis of Nerve Agent VX

Eric V. Patterson and Christopher J. Cramer*

Department of Chemistry and Supercomputer Institute, University of Minnesota, 207 Pleasant St SE, Minneapolis, Minnesota 55455-0431, USA

Received 27 June 1997; revised 11 August 1997; accepted 12 August 1997

ABSTRACT: The P—S bond cleavage process in the hydroperoxidolysis of a model system for the nerve agent VX was studied using *ab initio* and semiempirical molecular orbital methods. Aqueous solvation effects were included through single-point calculations using the semiempirical SM5.2PD/A continuum solvation model and geometries optimized at the HF/MIDI! level of theory. The predominant pathway for P—S bond cleavage involves pseudorotation of a low-energy trigonal bipyramidal intermediate followed by apical ligand ejection. In aqueous solution, the free energy barriers for these processes are found to be 14.3 and 4.6 kcal mol^{-1}, respectively, with electronic energies calculated at the MP2/cc-pVDZ//HF/MIDI! level of theory. By comparison with another continuum model of solvation (PCM), it is concluded that the SM5.2PD/A model performs well even for hypervalent phosphorus species, in spite of not having included any such molecules in the model's parameterization set. © 1998 John Wiley & Sons, Ltd.

KEYWORDS: P—S bond cleavage; hydroperoxidolysis; nerve agent VX; molecular orbital calculations

Additional material for this paper is available from the epoc website at http://www.wiley.com/epoc

INTRODUCTION

Most chemical nerve agents are phosphorus(V) species, which act as acetylcholinesterase inhibitors.[1] Present military doctrine calls for bulk field decontamination of nerve agents via hydrolysis in organic or aqueous media, and this goal has been the focus of considerable attention.[2–24] Many of these agents, belonging to the so-called G-series, contain only P—O, P—C and P—F bonds. These G-series agents are readily detoxified by aqueous hydroxide ion, at least on a small scale. During detoxification, the P—F bond is hydrolyzed, leaving behind a non-toxic phosphonic acid. The mechanism for this detoxification has been generally assumed to proceed through a trigonal bipryramidal phosphorus species,[25–32] although direct nucleophilic displacement of fluoride by hydroxide is also possible.

If a stable trigonal bipyramidal species is formed, several pseudorotamers are possible.[33,34] The stability of a particular pseudorotamer depends upon many factors, including the apicophilicity of the various ligands (correlated with electronegativity) and a ligand's ability to hyperconjugate with the central phosphorus atom.[25,35–49] Elimination from trigonal bipyramidal species is typically most facile from apical positions, and hence apicophilic ligands tend to be good leaving groups.[35] Since fluorine is the most electronegative element, it is strongly apicophilic, and it is the preferred leaving group in the reaction of G-series nerve agents with hydroxide.

VX [*O*-ethyl *S*-(2-diisopropylamino)ethyl methylphosphonothioate] differs from the G-agents in that it contains a P—S bond, which makes this exceedingly toxic, non-volatile, viscous material resistant to decontamination by aqueous hydroxide ion.[2,3,18,20,21] Thus, the fluoride ligand of the G-series agents has been replaced by a *β*-*N*,*N*-dialkylaminothiolate in VX.

This thiolate is expected to be less apicophilic than either the ethoxide or hydroxide ligands, the latter two of which are expected to have similar apicophilicities. As a result, no single ligand dominates for elimination, and two products are formed when VX reacts with hydroxide ion (Scheme 1). The thioester resulting from ethoxide loss is less toxic than VX, but is still a significant biohazard, and is moreover resistant to further hydrolysis.

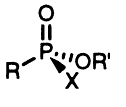

G series
R,R' = alkyl
X = F or CN

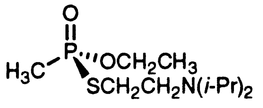

VX

**Correspondence to:* C. J. Cramer, Department of Chemistry and Supercomputer Institute, University of Minnesota, 207 Pleasant St SE, Minneapolis, Minnesota 55455-0431, USA. E-mail: cramer@chem.umn.edu

Contract/grant sponsor: United States Army Research Office.
Contract/grant sponsor: Alfred P. Sloan Foundation.

CCC 0894–3230/98/040232–09 $17.50

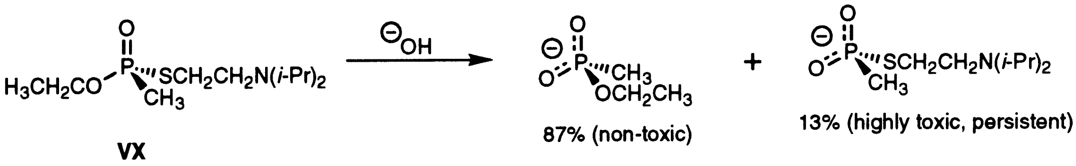

Scheme 1

Nucleophiles other than hydroxide have shown greater promise for the complete detoxification of VX, and function either by compartmentalizing the nerve agent in a micelle (or other medium) for convenient reagent delivery and disposal, or by shifting the equilibrium to afford complete P—S bond cleavage. An effective reagent in the first regard is *o*-iodosobenzoic acid,[12–14,19,22,50] while aqueous perhydroxide ion has shown promise for the latter.[21]

Yang *et al.*[21] have demonstrated that aqueous perhydroxide ion reacts with VX 40 times faster than aqueous hydroxide ion. More importantly, perhydrolysis selectively cleaves the P—S bond, leading to a non-toxic phosphonate as the sole observable product. The short half-life of this reaction (42 sec, compared with 31 min for VX reacting with hydroxide) and the non-toxicity of the final products make perhydrolysis a candidate for battlefield decontamination of VX. However, there are unanswered questions concerning the mechanism of neutralization.

Two likely pathways, diverging upon formation of a trigonal bipyramidal intermediate by nucleophilic addition, have been proposed for the perhydrolysis of VX. Scheme 2 depicts these pathways (and an additional pathway not considered by Yang *et al.*[18]) for a model compound that retains the key features of VX but is more tractable for the computational studies described herein. One possibility (path 1) is proposed to proceed via a pseudorotamer which places the perhydroxide and ethoxide (here modeled by F) ligands in the apical positions (assuming that electronegativity dominates apicophilicity, pseudorotamer **TBP1** will be favored over alternative **TBP2**, as alkoxy groups are more electronegative than thiolate groups), and involves a 1,2-thiolate shift to create a sulfenate phosphonoanhydride (a mechanism resembling a Baeyer–Villiger oxidation), the latter being especially susceptible to further hydrolysis.

A defining feature of the overall reaction, however, is that no experimental evidence for P—O cleavage is found. Since ligand elimination generally occurs more rapidly from apical rather than equatorial positions in pentacoordinate phosphorus species, and since **TBP1** is expected to be the most stable pentacoordinate intermediate, one might expect P—O cleavage to compete with P—S cleavage in the perhydrolysis. Three possible explanations for the lack of ethoxide loss may be offered. First, the 1,2-thiolate shift may simply occur much more rapidly than alkoxide elimination (a possibility with some precedence in the non-aqueous oxidation of thiolate pesticide derivatives[51–53]). Alternatively, loss of the thiolate ligand may be facile from an *equatorial* position of **TBP1** (path 2 in Scheme 2). Finally, apical elimination of thiolate from the alternative pseudorotamer **TBP2** may proceed with a sufficiently low barrier that path 3 in Scheme 2 becomes the preferred process, even though in the absence of unusual hyperconjugative interactions,[45] one would expect **TBP2** to be higher in energy than **TBP1**.

In an effort to clarify the details of the P—S cleavage

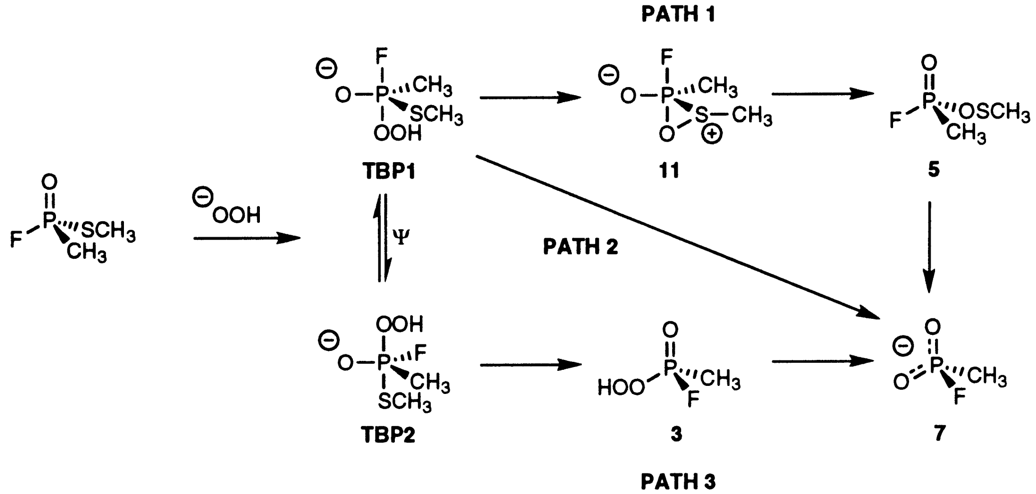

Scheme 2

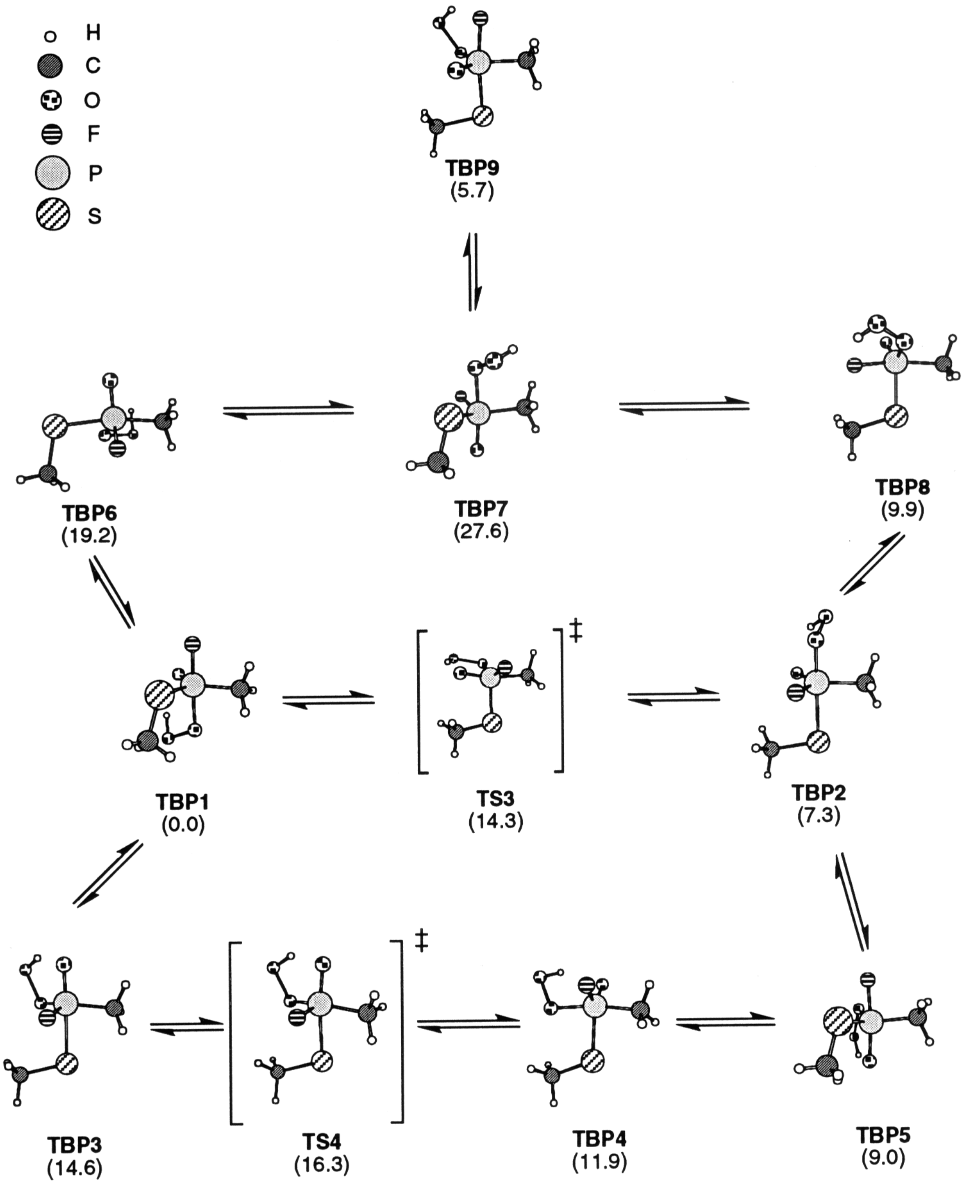

Figure 1. Free energies (kcal mol^{-1}) relative to **TBP1** and connectivity for all stationary points located on the pseudorotational potential energy surface in aqueous solution

step in the perhydrolysis of VX, we employed *ab initio* molecular orbital calculations, taking into account aqueous solvation effects. Since VX is an unwieldy molecule by *ab initio* standards, we adopted a simplified model. In this model, we reduced the computational cost by replacing the *S*-diisopropylaminoethyl chain with a simple thiomethyl group and the ethoxide ligand with a fluoride. The removal of the amino chain is unlikely to affect our results as they relate to pseudorotational equilibria and P—S bond cleavage barriers. The presence of a fluoride ligand in place of an alkoxy group may influence the pseudorotational equilibrium, but we expect this effect to be unimportant for the issues studied here—future work will focus on this point more closely. Our goal, then, was to clarify some of the mechanistic details of P—S bond cleavage during the reaction of nerve agent VX with aqueous perhydroxide ion.

Of course, mechanisms other than those discussed above may also be envisioned. For instance, hydrogen peroxide homolysis could initiate free radical reactions, but this seems unlikely in a basic aqueous medium. In the case of reaction with peroxy acids, the initial step in VX detoxification appears to be oxidation at sulfur followed by hydrolytic P—S cleavage,[24] but we expect the hydroperoxide anion to be more potent as a nucleophile under the relevant experimental conditions than as an oxidant. Finally, an S_N2 attack of the hydroperoxide nucleophile on the carbon of the thiomethyl ligand might be a concern were the computational model compound to be subjected to the experimental conditions; since this

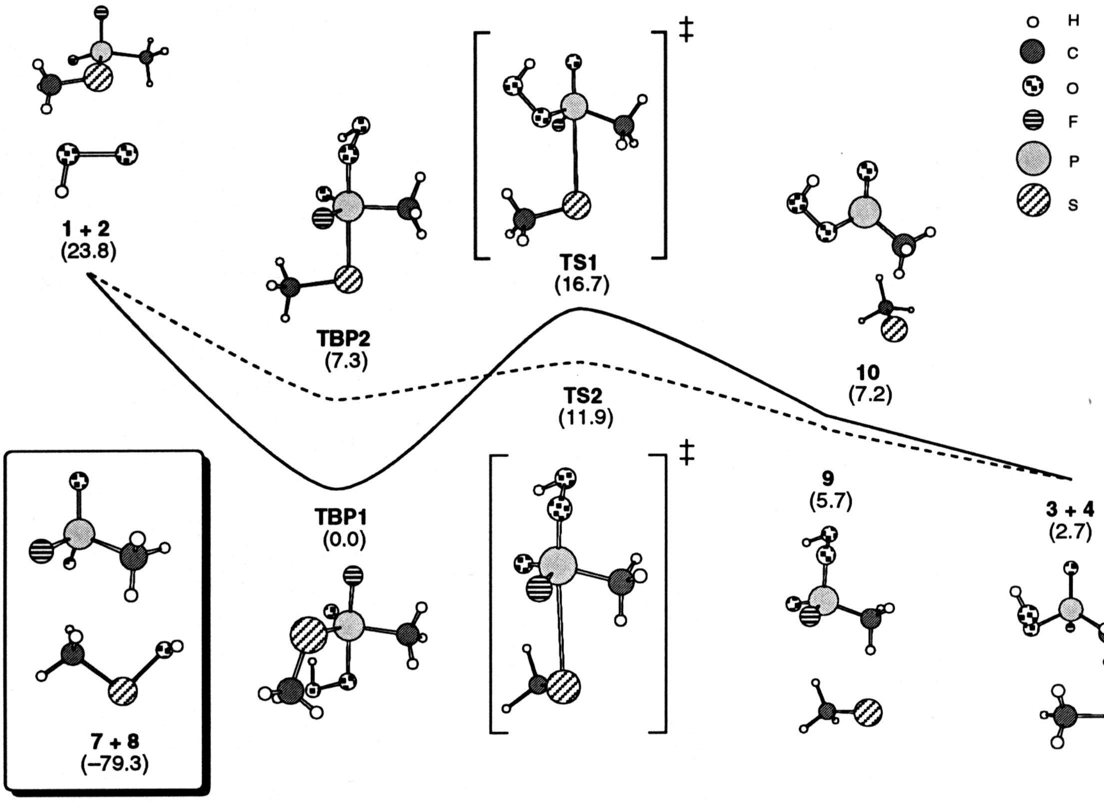

Figure 2. Free energies (kcal mol^{-1}) relative to **TBP1** for competing P—S cleavage pathways in aqueous solution

carbon is significantly more crowded in VX and no experimental evidence supports such reactivity, we do not examine such a pathway here.

COMPUTATIONAL METHODS

Ideally, for a reaction taking place in aqueous solution, solvation effects should be included during all phases of the calculation. However, the current state-of-the-art makes *ab initio* geometry optimizations in the condensed phase prohibitively expensive for systems of the size studied here. We therefore relied on a hybrid method of gas-phase optimizations followed by single-point calculations of the free energy of aqueous solvation to obtain final free energies in solution.

All geometries in this study were fully optimized using *ab initio* molecular orbital theory employing Hartree–Fock theory and the MIDI! basis set (HF/MIDI!). The MIDI! basis set[54] is an extension of the MIDI basis set[55] designed to provide geometries and partial charges (the latter critical for the calculation of solvation free energies) that compare well with results obtained from higher levels of theory (e.g. MP2/cc-pVDZ) but at greatly reduced cost for, *inter alia*, molecules containing phosphorus. Analytical frequencies confirmed the nature of all stationary points as either minima or transition states. Intrinsic reaction coordinate (IRC) calculations[56,57] were carried out to establish the two minima connected by every transition state. Single-point energy calculations at the HF/MIDI! optimized geometries were performed using second-order Møller–Plesset perturbation theory[58] (MP2) and the larger cc-pVDZ basis set[59] (MP2/cc-pVDZ//HF/MIDI!). Including thermal corrections from the HF/MIDI! frequency calculations, our best gas-phase energy is described as MP2/cc-pVDZ//HF/MIDI! $+ G^{298}{}_{\text{gas}}$. All gas-phase calculations were performed using the Gaussian 94[60] suite of electronic structure programs.

Aqueous solvation was accounted for by two different approaches. We used a version of HONDO 7[61] including the polarized continuum model (PCM) of Tomasi and co-workers[62,63,64] to perform single-point solvation free energy calculations on the HF/MIDI!-optimized structures at both the HF/MIDI! and MP2/MIDI! levels. We also performed single-point aqueous solvation free energy calculations using the SM5.2PD/A aqueous solvation model in a locally modified version of AMSOL 5.4.1.[65] All solvation calculations were performed for a temperature of 298 K.

RESULTS AND DISCUSSION

Figures 1 and 2 depict all minima and transition states studied on the potential energy surfaces for pseudorota-

Table 1. Free energies of solvation (kcal mol^{-1}) at 298 K for all species considered in this study at HF/MIDI! geometries

	PCM-HF/MIDI!			PCM-MP2/MIDI!			SM5.2PD/A		
Species	ΔG_{EP}[a]	G_C[b]	ΔG_S[c]	ΔG_{EP}[a]	G_C[b]	ΔG_S[c]	ΔG_{EP}[a]	G_{CDS}[d]	ΔG_S[c]
1	−11.1	17.3	6.2	−8.5	17.3	8.8	−1.8	−4.9	−6.7
2	−90.9	6.7	−81.2	−91.8	6.7	−85.2	−87.6	−8.2	−95.9
3	−12.8	14.4	1.6	−10.3	14.4	4.0	−2.0	−7.8	−9.8
4	−66.9	10.4	−56.6	−66.6	10.4	−56.3	−70.0	−5.1	−75.1
5	−11.5	18.6	7.2	−9.2	18.6	9.4	−2.3	−5.3	−7.6
6	−99.9	−4.8	−95.1	−99.9	4.8	−95.1	−100.3	−9.2	−109.5
7	−69.9	12.6	−57.2	−67.4	12.6	−54.7	−71.0	−8.6	−79.6
8	−7.3	11.6	4.3	−6.6	11.6	5.0	−1.2	−6.4	−7.7
9	−59.3	22.7	−36.6	−57.5	22.7	−34.7	−62.6	−10.5	−73.1
10	−59.5	22.2	−37.3	−57.7	22.2	−35.5	−62.4	−9.9	−72.3
TBP1	−63.3	19.5	−43.8	−60.7	19.5	−41.2	−60.7	−6.5	−67.1
TBP2	−60.2	19.9	−40.3	−58.2	19.9	−38.3	−58.9	−6.8	−65.7
TBP3	−60.0	19.8	−40.2	−58.2	19.8	−38.3	−60.3	−6.2	−66.4
TBP4	−61.7	19.7	−42.0	−59.8	19.7	−40.2	−58.3	−5.9	−64.2
TBP5	−61.3	19.8	−41.5	−59.1	19.8	−39.3	−58.3	−6.0	−64.3
TBP6	−63.6	20.2	−43.4	−61.5	20.2	−41.3	−57.5	−8.6	−66.2
TBP7	−67.2	19.8	−47.4	−64.3	19.8	−44.5	−58.9	−6.7	−65.6
TBP8	−63.9	19.8	−44.2	−61.8	19.8	−42.0	−57.3	−9.1	−66.4
TBP9	−62.6	19.9	−42.8	−60.4	19.9	−40.6	−57.6	−7.8	−65.4
TS1	−59.9	21.2	−38.7	−57.6	21.2	−36.4	−61.9	−7.2	−69.0
TS2	−59.6	21.5	−38.2	−57.6	21.5	−36.1	−62.4	−7.8	−70.2
TS3	−62.1	19.8	−42.3	−59.9	19.8	−40.1	−60.5	−5.8	−66.3
TS4	−59.7	19.8	−39.9	−58.0	19.8	−38.2	−59.9	−5.9	−65.8

[a] Electostatic polarization contribution.
[b] Cavitation contribution.
[c] Total free energy of solvation, i.e. sum of ΔG_{EP} and G_C or G_{CDS}.
[d] Contribution from cavitation, dispersion and solvent structural reorganization.

tion of the trigonal bipyramidal intermediates and loss of the methanethiolate fragment, respectively. Cartesian coordinates for HF/MIDI!-optimized geometries are provided as supplementary material on the EPOC website at http://www.wiley.com/epoc. Aqueous free energies of solvation as calculated at three different levels of theory (see below) are listed for all stationary points in Table 1. Relative free energies for each stationary point along the complete potential energy surface, in the gas phase and aqueous solution, are presented in Table 2. Where necessary, sums of individual fragments were used in Table 2 to ensure balanced comparisons, e.g. the free energies of VX model **1** and the hydroperoxide ion (**2**) have been summed for direct comparison with the trigonal bipyramidal intermediates.

This section continues with a discussion of three issues, one technical and the other two chemical. First, we examine the relative utility of the PCM and SM5.2PD/A solvation models for the calculation of aqueous solvation effects. Next, we consider the implications of our calculations for the mechanism of perhydrolysis of VX, focusing first on the pseudorotational equilibrium of the pentacoordinate phosphorus intermediates and second on P—S bond cleavage.

Comparison of solvation models

Typical molecular orbital calculations are for isolated molecules in the gas phase at 0 K. Results from such calculations may sometimes be compared semiquantitatively with those of condensed-phase experiments, provided that solvent effects are minimal (which is almost never true for charged systems). Since the perhydrolysis of VX involves anionic species in aqueous solution, the effects of solvation are expected to be large (as noted previously for the hydrolysis of phosphate esters,[66–69] for instance). Indeed, the results in Table 1 confirm this to be the case. Regardless of solvation model, the electrostatic contribution to the total free energy of solvation is fairly large for all anionic species (**2, 4, 6, 7**, all of the trigonal bipyramidal intermediates (TBPs) and all of the transition states). For the smallest anions, the free energy of solvation ranges as high as 100 kcal mol^{-1} (1 kcal = 4.184 kJ). For the larger anionic species, the charge delocalizes over a larger volume, so the free energies of solvation are reduced in magnitude, but still range as high as 70 kcal mol^{-1}. The free energy of solvation is similarly large in the ion–dipole complexes **9** and **10** (discussed further below), where

Table 2. Relative free energies (kcal mol^{-1}) of points along the potential energy surface (298 K)

Species	Gas phase[a]	$\Delta\Delta G_{sol}$ (aqueous solution) PCM-MP2[b]	$\Delta\Delta G_{sol}$ (aqueous solution) SM5.2PD/A[b]
1 + **2**	49.3	24.1	23.8
3 + **4**	20.5	9.4	2.7
5 + **6**	33.6	−10.1	−15.6
7 + **8**	−59.1	−67.6	−79.3
9	10.9	18.2	5.7
10	11.6	18.1	7.2
TBP1	0.0[c]	0.0	0.0
TBP2	5.9	8.8	7.3
TBP3	13.9	16.8	14.6
TBP4	9.0	10.0	11.9
TBP5	6.2	8.1	9.0
TBP6	18.3	18.2	19.2
TBP7	26.1	22.8	27.6
TBP8	9.2	8.4	9.9
TBP9	4.0	4.6	5.7
TS1	18.6	23.4	16.7
TS2	15.0	20.1	11.9
TS3	13.5	14.6	14.3
TS4	15.0	18.0	16.3

[a] MP2/cc-pVDZ/HF/MIDI! electronic energy + 298 K thermal corrections.

[b] Gas-phase $\Delta\Delta G$ + indicated solvation free energy correction.

[c] Absolute energy (au) HF/MIDI!, −1136.22148; MP2/cc-pVDZ//HF/MIDI!, −1143.41743; thermal correction (298 K HF/MIDI!), 0.07681.

significant charge polarization has developed in the separating fragments. The remaining species, all neutral, have much smaller free energies of solvation, as expected.

Although Table 2 indicates the shape of the gas-phase potential energy surface to be qualitatively correct, solvation effects differentially impact neutral and anionic species (the latter being stabilized much more strongly). Solvation effects further discriminate compact anions [e.g. perhydroxide (**2**) and hydroxide (**6**)] from less compact anions (e.g. the TBPs). The set of relative free energies in aqueous solution should be more consistent with experimental observations.

Ideally, aqueous solvation effects would be included during the geometry optimization process, since it is possible that the solvated equilibrium geometries will vary significantly from their corresponding gas-phase minima.[70,71] However, various considerations render this impractical here. Condensed-phase optimizations using the PCM model in HONDO 7 are done numerically, and tend to be cumbersome (an optimization of hydroxide ion in water required more than 30 min of CPU time on a modern workstation). SM5.2PD/A optimizations, on the other hand, are fast but are contraindicated here because the AM1 Hamiltonian[72–75] on which the model is based is inappropriate for evaluating the geometries of hypervalent phosphorus species. This is not, however, expected to impact adversely the quality of the SM5.2PD/A solvation free energies, which employ the AM1 Hamiltonian only for generating a charge distribution, not for molecular energies. Indeed, the SM5.2PD/A and the *ab initio* PCM electrostatic free energies of solvation (ΔG_{EP} columns in Table 1) agree well with each other for identical HF/MIDI! geometries.

Care must be exercised in further comparing the two solvation models. Currently available *ab initio* continuum solvation models typically treat only the effects of electrostatic polarization on the energy of the system (ΔG_{EP}) However, for a solvation model to be quantitatively accurate, non-electrostatic terms must also be accounted for. These terms include cavitation (the cost for making a hole in the solvent for the solute), dispersion (attractive London forces) and solvent structural rearrangement (e.g. the hydrophobic effect); these sum to G_{CDS}. The PCM model in HONDO 7 includes terms for cavitation[76] and dispersion,[77] but the latter requires Caillet–Claverie parameters[77] for each atom in the solute, so we employed only the cavitation correction. The final ΔG_{sol} arrived at by adding ΔG_{EP} and G_C thus neglects dispersion and solvent structural rearrangements and, while unlikely to compare well with experimental free energies of solvation, is still perhaps appropriate for computing relative free energies.

The SM*x* family of aqueous solvation models,[78–81] on the other hand, parametrically includes all of the above-discussed effects in calculating the total solvation free energy. These models usually are in good agreement with experimental free energies of solvation for organic solutes and numerous examples of the predictive power of the SM*x* models exist in the literature for conformational[82–93] and tautomeric[82,94–97] equilibria. The SM5.2PD/A model[81] employed for this work has a mean unsigned error of 0.5 kcal mol^{-1} for a set of over 200 organic solutes. Examination of Table 1 indicates that the ΔG_{EP} terms obtained from SM5.2PD/A and PCM compare well in most cases, particularly for the anions. The PCM G_C terms, on the other hand, are necessarily always positive, but still correlate reasonably with the SM5.2PD/A G_{CDS} terms. Hence, while the *absolute* free energies from SM5.2PD/A are expected to the more accurate, the *relative* solvation free energies from both models are overall comparable (in part because the electrostatic polarization effect dominates for charged species, so differences in CDS are less important). This agreement between two different continuum approaches inspires confidence in the final results (Table 2).

We note a few more technical points in closing this section. First, the generally good agreement between SM5.2PD/A and PCM on ΔG_{EP} for hypervalent phosphorus species suggests that the former model is applicable to these systems in spite of not having included any in its parameterization set. This result is in line with previous work[69] showing the good agreement between another SM*x* model (SM3.1[98]) and finite difference Poisson calculations[66] of the electrostatic free energies of solvation for pentacoordinate intermediates in phosphate hydrolysis. Second, the computational cost of the SM5.2PD/A single points is roughly four orders of magnitude less than for PCM. Finally, we note that the similarity between PCM-HF and PCM-MP2 calculations suggests that there is no special synergism between solvation effects and electron correlation. All further discussion of relative energies will be for aqueous solution and will focus on the SM5.2PD/A results, which we consider to be both the most accurate and the most economical.

Trigonal bipyramids

The first step in the overall mechanism is attack at phosphorus by hydroperoxide ion. We find this step to proceed without barrier to any of a number of TBPs. To understand the mechanism, it is vital to understand the relationships among the various TBPs. With five unique ligands, 10 enantiomeric pairs of TBPs may be envisioned (neglecting possible conformational isomerism associated with the ligands themselves); it is, of course, not required that all 10 be stable intermediates. Those which *are* stable can in principle interconvert via pseudorotation.[33,34] Stationary points corresponding to all 10 possible pseudorotamers were located. One of these 10, with oxide and methyl groups apical, is a transition state (**TS3**), presumably due to the lack of electronegative atoms in the apical positions.

Not surprisingly, the lowest energy TBP is **TBP1**, with the fluoride and hydroperoxide ligands in the apical positions (Figure 1). This TBP is analogous to one of the two important TBP intermediates suggested (Scheme 2) by Yang *et al.*[21] and we shall define the energies of all other species relative to it as zero (Table 2). Although **TBP1** is the most stable TBP, it does lie 79.3 kcal mol^{-1} above the final products (**7** and **8**). **TBP2,** with perhydroxide and methanethiolate in the apical positions, is analogous to the other important TBP intermediate suggested by Yang *et al.* **TBP2** lies 7.3 kcal mol^{-1} above **TBP1.** We located the transition state for interconversion of these two pseudorotamers, **TS3.** Interestingly, the transition state corresponds to the one TBP that is not an energy minimum as noted above. Therefore, interconversion of **TBP1** and **TBP2** occurs via a double Berry pseudorotation;[33,34] the first half of the pseudorotation takes **TBP1** to **TS3** and the second half transforms **TS3** into **TBP2.** The barrier to pseudorotation from **TBP1** to **TBP2** is found to be 14.3 kcal mol.$^{-1}$

We located the seven remaining TBPs and found that all are higher in energy than **TBP2,** although most are clustered less than 20 kcal mol^{-1} above **TBP1.** Only **TBP7** lies significantly higher than the others, being nearly 30 kcal mol^{-1} higher in energy than **TBP1.** Again, standard electronegativity arguments can be used to explain satisfactorily the relative stabilities of each TBP, although the importance of hyperconjugation vs apicophilicity has not been investigated in this case,[45] and cannot be ruled out. We also located one additional transition state (**TS4**), for the interconversion of **TBP3** to **TBP4.** This transition state is the standard square pyramidal structure expected for a single Berry pseudorotation, and results in a modest barrier of 1.7 kcal mol^{-1} from **TBP3** to **TBP4.**

An examination of the potential energy surface for pseudorotation (Figure 1) shows that the double pseudorotation from **TBP1** to **TBP2** is the lowest energy pathway to interconvert the two TBPs of greatest interest. Although complete characterization of all transition state structures on the pseudorotational potential energy surface has not been carried out, it is clear that the other two possible pathways shown in Figure 1 will both require higher activation energies than the 14.3 kcal mol^{-1} required to take **TBP1** through **TS3** to **TBP2.** We note that we have not made any effort here to account for possible dynamic effects and their potential influence on reaction trajectories; however, given the complex motions involved here in traversing the potential energy surface from one TBP to another, we do not expect dynamic effects to play as significant a role as barrier heights in determining the reaction path. We next examine the energetics of P—S bond cleavage from the low-energy TBPs **TBP1** and **TBP2.**

P—S bond cleavage

By conventional logic, cleavage of the P—S bond is most likely to occur when the methanethiolate ligand is in an apical position.[35] **TBP2** is the lowest energy TBP with the thiolate so disposed. The transition state (**TS1**) for apical loss of methanethiolate (**4**) lies 4.6 kcal mol^{-1} above **TBP2** (Figure 2), and connects it to an ion–dipole complex (**9**) in which the methanethiolate group is loosely associated with the phosphonate ester. This contact intermediate, which is nearly isoenergetic with **TBP2,** may be an artifact of gas-phase optimization, as the electrostatic forces which hold this structure together are expected to be weak in an aqueous environment. From intermediate **9,** the reaction proceeds without significant barrier to fully separated intermediates **3** and **4,** which lie 4.6 kcal mol^{-1} below **TBP2.** These species then presumably undergo reduction and oxidation, respectively, to generate **7** and **8** (and indeed, the final fate of the methanethiolate under the reaction conditions is likely to be conversion to methanesulfonic acid).

We also performed a search for a transition state structure corresponding to equatorial elimination of methanethiolate from **TBP1.** Not surprisingly, the barrier for this process is significantly higher (16.7 kcal mol^{-1}) than for apical elimination. In fact, a pseudorotation occurs during ligand ejection, so that the thiolate ligand is in an apical position by the time **TS2** is reached. As in direct apical loss, this pathway passes through an electrostatically bound ion–dipole complex (**10**) before passing on to final products **3** and **4,** which lie slightly higher in energy than **TBP1.**

It is important and informative to compare the barriers for ligand loss to the barrier for pseudorotation between **TBP1** and **TBP2.** To pseudorotate, **TBP1** needs 14.3 kcal mol^{-1} compared with the 16.7 kcal mol^{-1} needed for P—S cleavage. Under thermodynamic control, this difference of 2.4 kcal mol^{-1} is sufficient to favor pseudorotation over ligand ejection by nearly two orders of magnitude at 298 K. Therefore, **TBP1** will pseudorotate to **TBP2** in preference to expelling **4.** Moreover, **TBP2** requires 7.0 kcal mol^{-1} to pseudorotate back to **TBP1** but only 4.6 kcal mol^{-1} to eject ligand **4.** Again, the energy difference is 2.4 kcal mol,$^{-1}$ and **TBP2** will preferentially cleave the P—S bond rather than pseudorotate back to **TBP1.** These results suggest that even if **TBP1** is first formed, it can easily pseudorotate to **TBP2** and eliminate methanethiolate (**4**). While the absolute energetics for the above-discussed processes as calculated by the PCM model are quantitatively different (as a result of failing to include the energetic effects of dispersion and solvent structural rearrangement), they agree that the lowest energy pathway for P—S bond cleavage is via apical loss from **TBP2** (Table 2).

We have been unable to locate a stationary point corresponding to cyclic structure **11** in Scheme 2. We have located the minimum (**5**) resulting from loss of hydroxide (**6**) and thiolate migration. We have been unsuccessful, however, in locating any stationary points connecting **5** and **6** to **TBP1.** We can make no definitive statements on this process, but speculate based on our results so far that this pathway requires significantly more energy than direct pathways for P—S bond cleavage. Attempts to locate connecting stationary points while including the effects of solvation are proceeding.

Future efforts will also examine competing P—O and P—S cleavage. To address this issue, we are considering systems where the fluorine in our current model is replaced with an alkoxide.

CONCLUSIONS

Molecular orbital calculations on the P—S cleavage step during the perhydrolysis of a VX nerve agent model indicate that the most stable trigonal bipyramidal intermediate has the thiolate in an equatorial position, from which the barrier to P—S cleavage is 16.7 kcal mol^{-1}. However, that trigonal bipyramid pseudorotates to a higher energy conformer with a barrier of only 14.3 kcal mol.$^{-1}$ Loss of methanethiolate from the latter is facile, with a barrier of only 4.6 kcal mol.$^{-1}$ These details help clarify certain aspects of the experimental results of Yang *et al.*[18] Further work with an improved model system will be necessary to address competitive P—O cleavage and to investigate alternative mechanistic pathways. As a technical point, the SM5.2PD/A continuum solvation model has been shown to provide reasonable aqueous free energies of solvation for pentacoordinate phosphorus species.

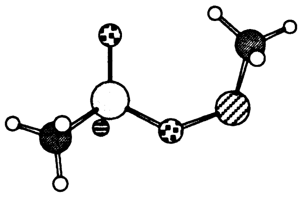

5

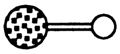

6

Acknowledgments

We are grateful for high-performance vector and parallel computing resources made available by the Minnesota Supercomputer Institute and the University of Minnesota–IBM Shared Research Project, respectively. Funding was provided by the United States Army Research Office and the Alfred P. Sloan Foundation. We thank Dr Laura Coitiño for technical assistance with the PCM model as implemented in HONDO 7.

REFERENCES

1. H. P. Benschop and L. P. A. de Jong. *Acc. Chem. Res.* **21,** 368 (1988).
2. A. H. Aharoni and R. D. O'Brien. *Biochemistry* **7,** 1538 (1968).
3. J. Epstein, J. J. Callahan and V. E. Bauer. *Phosphorus* **4,** 157 (1974).
4. J. H. Fendler and E. J. Fendler. *Catalysis in Micellar and Micromolecular Systems,* p. 150. Academic Press, New York (1975).
5. E. Buncel, H. Wilson and B. Chuaqui. *J. Am. Chem. Soc.* **104,** 4896 (1982).
6. C. A. Bunton, L.-H. Gan and G. Savelli. *J. Phys. Chem.* **87,** 5491 (1983).
7. C. A. Bunton, M. M. Mhala, J. R. Moffatt, D. Monarres and G. Savelli. *J. Org. Chem.* **49,** 426 (1984).
8. R. A. Moss, S. Swarup, T. F. Hendrickson and Y. Z. Hui. *Tetrahedron Lett.* **25,** 4079 (1984).
9. M. L. Cordeiro, D. L. Pompliano and J. W. Frost. *J. Am. Chem. Soc.* **108,** 332 (1986).
10. L. Z. Avila, S. H. Loo and J. W. Frost. *J. Am. Chem. Soc.* **109,** 6758 (1987).
11. J. W. Frost, S. Loo, M. L. Cordeiro and D. Li. *J. Am. Chem. Soc.* **109,** 2166 (1987).
12. B. A. Burnside, B. L. Knier, R. A. Mackay, H. D. Durst and F. R. Longo. *J. Phys. Chem.* **92,** 4505 (1988).
13. R. A. Moss, D. Bolikal, H. D. Durst and J. W. Hovanec. *Tetrahedron Lett.* **29,** 2433 (1988).
14. R. A. Moss, Y.-C. Chung, H. D. Durst and J. W. Hovanec. *J. Chem. Soc., Perkin Trans. 1* 1350 (1989).
15. P. S. Hammond, J. S. Forster, C. N. Lieske and H. D. Durst. *J. Am. Chem. Soc.* **111,** 7860 (1989).
16. K. E. DeBruin, C. W. Tang, D. M. Johnson and R. L. Wilde. *J. Am. Chem. Soc.* **111,** 5871 (1989).

17. C. A. Bunton, M. M. Mhala and J. R. Moffatt. *J. Phys. Org. Chem.* **3,** 390 (1990).
18. Y.-C. Yang, L. L. Szafraniec, W. T. Beaudry and D. K. Rohrbaugh. *J. Am. Chem. Soc.* **112,** 6621 (1990).
19. C. A. Panetta, S. M. Garlick, H. D. Durst, F. R. Longo and J. R. Ward. *J. Org. Chem.* **55,** 5202 (1990).
20. Y. C. Yang, J. A. Baker and J. R. Ward. *Chem. Rev.* **92,** 1729 (1992).
21. Y.-C. Yang, L. L. Szafraniec, W. T. Beaudry and C. A. Bunton. *J. Org. Chem.* **58,** 6964 (1993).
22. R. A. Moss and H. Zhang. *J. Am. Chem. Soc.* **116,** 4471 (1994).
23. D. R. Leslie and S. Pantelidis. *Aust. J. Chem.* **47,** 545 (1994).
24. A. Blaskó, C. A. Bunton and A. Kumar. *J. Phys. Org. Chem.* **10,** 427 (1997).
25. F. H. Westheimer. *Acc. Chem. Res.* **1,** 70 (1968).
26. F. H. Westheimer. *Science* **237,** 1173 (1987).
27. A. Fersht. *Enzyme Structure and Mechanism.* Freeman, New York (1985).
28. P. C. Haake and F. H. Westheimer. *J. Am. Chem. Soc.* **83,** 1102 (1961).
29. J. R. Cox and B. Ramsay. *Chem. Rev.* **64,** 317 (1964).
30. R. Kluger, F. Covitz, E. Dennis, L. D. Williams and F. H. Westheimer. *J. Am. Chem. Soc.* **91,** 6066 (1969).
31. J. Emsley and D. Hall. *The Chemistry of Phosphorus,* p. 494. Wiley, New York (1976).
32. R. R. Holmes. *J. Am. Chem. Soc.* **100,** 433 (1978).
33. R. S. Berry. *J. Chem. Phys.* **32,** 933 (1960).
34. K. Mislow. *Acc. Chem. Res.* **3,** 321 (1970).
35. G. R. J. Thatcher and R. Kluger. *Adv. Phys. Org. Chem.* **25,** 99 (1989).
36. E. L. Muetterties, W. Mahler and R. Schmutzler. *Inorg. Chem.* **2,** 613 (1963).
37. R. S. McDowell and A. Streitwieser. *J. Am. Chem. Soc.* **107,** 5849 (1985).
38. J. A. Deiters, R. R. Holmes and J. M. Holmes. *J. Am. Chem. Soc.* **110,** 7672 (1988).
39. P. Wang, D. K. Agrafiotis, A. Streitwieser and P. v. R. Schleyer. *J. Chem. Soc., Chem. Commun.* 201 (1990).
40. C. J. Cramer. *J. Am. Chem. Soc.* **112,** 7965 (1990).
41. C. J. Cramer. *J. Am. Chem. Soc.* **113,** 2439 (1991).
42. P. Wang, Y. Zhang, R. Glaser, A. E. Reed, P. v. R. Schleyer and A. Streitwieser. *J. Am. Chem. Soc.* **113,** 55 (1991).
43. H. Wasada and K. Hirao. *J. Am. Chem. Soc.* **114,** 16 (1992).
44. C. J. Cramer. *Chem. Phys. Lett.* **202,** 297 (1993).
45. C. J. Cramer and S. M. Gustafson. *J. Am. Chem. Soc.* **115,** 9315 (1993).
46. P. Wang, Y. Zhang, R. Glaser, A. Streitwieser and P. v. R. Schleyer. *J. Comput. Chem.* **14,** 522 (1993).
47. C. J. Cramer and S. M. Gustafson. *J. Am. Chem. Soc.* **116,** 723 (1994).
48. S. M. Gustafson and C. J. Cramer. *J. Phys. Chem.* **99,** 2267 (1995).
49. B. D. Wladkowski, M. Krauss and W. J. Stevens. *J. Phys. Chem.* **99,** 4490 (1995).
50. S. M. Garlick, H. D. Durst, R. A. Mackay, K. G. Haddaway and R. F. Longo. *J. Colloid Interface Sci.* **135,** 508 (1990).
51. J. Bielawski and J. E. Casida. *J. Agric. Food Chem.* **36,** 610 (1988).
52. Y. Segall, S.-Y. Wu, R. F. Toia and J. E. Casida. *Tetrahedron Lett.* **31,** 473 (1990).
53. D. R. Leslie, W. T. Beaudry, L. L. Szafraniec and D. K. Rohrbaugh. *J. Org. Chem.* **56,** 3459 (1991).
54. R. E. Easton, D. J. Giesen, A. Welch, C. J. Cramer and D. G. Truhlar. *Theor. Chim. Acta* **93,** 281 (1996).
55. S. Huzinaga, J. Andzelm, M. Klobukowski, E. Radzio-Andzelm, Y. Sakai and H. Tatewaki. in *Gaussian Basis Sets for Molecular Calculations,* edited by S. Huzinaga. Elsevier, Amsterdam (1984).
56. N. Sathyamurthy. *Comp. Phys. Rep.* **3,** 1 (1986).
57. C. Gonzalez and H. B. Schlegel. *J. Chem. Phys.* **90,** 2154 (1989).
58. C. Møller and M. S. Plesset. *Phys. Rev.* **46,** 618 (1934).
59. T. H. Dunning. *J. Chem. Phys.* **90,** 1007 (1989).
60. M. J. Frisch, G. W. Trucks, H. B. Schlegel, P. M. W. Gill, B. G. Johnson, M. A. Robb, J. R. Cheeseman, T. Keith, G. A. Petersson, J. A. Montgomery, K. Raghavachari, M. A. Al-Laham, V. G. Zakrzewski, J. V. Ortiz, J. B. Foresman, J. Cioslowski, B. B. Stefanov, A. Nanayakkara, M. Challacombe, C. Y. Peng, P. Y. Ayala, W. Chen, M. W. Wong, J. L. Andres, E. S. Replogle, R. Gomperts, R. L. Martin, D. J. Fox, J. S. Binkley, D. J. Defrees, J. Baker, J. P. Stewart, M. Head-Gordon, C. Gonzalez and J. A. Pople. *Gaussian 94, Revision D.1.* Gaussian Pittsburgh, PA (1995).
61. Program No. 544 from the Quantum Chemistry Program Exchange.
62. S. Miertus, E. Scrocco and J. Tomasi. *Chem. Phys.* **55,** 117 (1981).
63. J. L. Pascual-Ahuir, E. Silla, J. Tomasi and R. Bonaccorsi. *J. Comput. Chem.* **8,** 778 (1987).
64. M. A. Aguilar and F. J. Olivares del Valle. *Chem. Phys.* **129,** 439 (1989).
65. C. J. Cramer, G. D. Hawkins, G. C. Lynch, D. J. Giesen, I. Rossi, J. W. Storer, D. G. Truhlar and D. A. Liotard. *QCPE Bull.* **15,** 41 (1995).
66. A. Dejaegere, C. Lim and M. Karplus. *J. Am. Chem. Soc.* **113,** 4353 (1991).
67. C. Lim and P. Tole. *J. Phys. Chem.* **96,** 5217 (1992).
68. P. Tole and C. Lim. *J. Am. Chem. Soc.* **116,** 3922 (1994).
69. C. J. Cramer, G. D. Hawkins and D. G. Truhlar. *J. Chem. Soc., Faraday Trans.* **90,** 1802 (1994).
70. C. Reichardt. *Solvents and Solvent Effects in Organic Chemistry.* VCH, New York (1990).
71. G. R. J. Thatcher and D. R. Cameron. *J. Chem. Soc., Perkin Trans.* 2 767 (1997).
72. M. J. S. Dewar, E. G. Zoebisch, E. F. Healy and J. J. P. Stewart. *J. Am. Chem. Soc.* **107,** 3902 (1985).
73. M. J. S. Dewar and E. G. Zoebisch. *J. Mol. Struct. (Theochem)* **180,** 1 (1988).
74. M. J. S. Dewar and C. Jie. *J. Mol. Struct. (Theochem)* **187,** 1 (1989).
75. M. J. S. Dewar and Y. Yate-Ching. *Inorg. Chem.* **29,** 3881 (1990).
76. R. A. Pierotti. *Chem. Rev.* **76,** 717 (1976).
77. J. Caillet, P. Claverie and A. Pullman. *Acta Cryst Callogr, Sect. B* **34,** 3266 (1978).
78. C. J. Cramer and D. G. Truhlar. *Science* **256,** 213 (1992).
79. C. J. Cramer and D. G. Truhlar. *J. Comput. Chem.* **13,** 1089 (1992).
80. C. J. Cramer and D. G. Truhlar. *J. Comput.-Aid. Mol. Des.* **6,** 629 (1992).
81. C. C. Chambers, G. D. Hawkins, C. J. Cramer and D. G. Truhlar. *J. Phys. Chem.* **100,** 16385 (1996).
82. C. J. Cramer and D. G. Truhlar. *J. Am. Chem. Soc.* **113,** 8552 9901(E) (1991).
83. C. J. Cramer. *J. Org. Chem.* **57,** 7034 (1992).
84. J. J. Urban, C. J. Cramer and G. R. Famini. *J. Am. Chem. Soc.* **114,** 8226 (1992).
85. C. J. Cramer and D. G. Truhlar. *J. Am. Chem. Soc.* **115,** 5745 (1993).
86. D. C. Lankin, N. S. Chandrakumar, S. N. Rao, D. P. Spangler and J. P. Snyder. *J. Am. Chem. Soc.* **115,** 3356 (1993).
87. R. A. Metcalfe, E. S. Dodsworth, A. B. P. Lever, W. J. Pietro and D. J. Stufkens. *Inorg. Chem.* **32,** 3581 (1993).
88. J. L. Asensio, R. López, A. Fernández-Mayoralas and J. Jiménez-Barbero. *Tetrahedron* **50,** 6417 (1994).
89. C. J. Cramer and D. G. Truhlar. *J. Am. Chem. Soc.* **116,** 3892 (1994).
90. W. L. Jorgensen, P. I. M. Detirado and D. L. Severance. *J. Am. Chem. Soc.* **116,** 2199 (1994).
91. S. Lovas and R. F. Murphy. *J. Mol. Struct. (Theochem)* **311,** 297 (1994).
92. D. L. Severance and W. L. Jorgensen. *J. Am. Chem. Soc.* **114,** 10966 (1992).
93. B. Yang, J. Wright, M. E. Eldefrawi, S. Pou and A. D. Mackerell. *J. Am. Chem. Soc.* **116,** 8722 (1994).
94. C. J. Cramer and D. G. Truhlar. *J. Am. Chem. Soc.* **115,** 8810 (1993).
95. J. G. Contreras and J. B. Alderte. *Bol. Sci. Chil. Quim.* **39,** 17 (1994).
96. D. W. Farnsworth, D. A. Wink, N. M. Roscher, C. J. Michejda and R. H. Smith. *J. Org. Chem.* **59,** 5942 (1994).
97. M. Orozco and F. J. Luque. *J. Am. Chem. Soc.* **117,** 1378 (1995).
98. D. A. Liotard, G. D. Hawkins, G. C. Lynch, C. J. Cramer and D. G. Truhlar. *J. Comput. Chem.* **16,** 422 (1995).